

K_{l3}^+ decays involving finite neutrino mass and mass mixing

R. R. L. Sharma* and N. K. Sharma

Department of Physics, University of Rajasthan, Jaipur-302004, India

(Received 11 October 1984)

K_{l3}^+ decays with the inclusion of effects of finite neutrino mass and mass mixing have been investigated. Predictions have been obtained for (i) pion energy spectrum, (ii) decay probability, (iii) $\pi-l$ ($=e,\mu$) angular correlations, (iv) $\pi-l$ energy correlations, (v) lepton energy spectrum, (vi) $\pi-\nu_i$ ($i=e,\mu,\tau$) angular correlations, and (vii) $\pi-\nu_i$ energy correlations. Finite-mass effects are substantial in all the parameters discussed, whereas the mixing effects are discernible only in $\pi-\nu_i$ angular and energy correlations. The mass limits for the ν_3 mass for hierarchical mixing are found to be 174.0 ± 0.9 MeV and 120 ± 2 MeV for electronic and muonic modes, respectively, with nearly identical values for Kobayashi-Maskawa mixing.

I. INTRODUCTION

At present, major efforts are being made to look for nonvanishing neutrino masses¹ and their mixings.²⁻⁵ A recent measurement by Boris *et al.*⁶ (with much improved energy resolution) of the near-end-point shape of the β spectrum in tritium decay puts a lower limit $m(\nu_e) > 20$ eV, whose upper limit is around⁷ 46 eV. The upper mass limits for ν_μ and ν_τ are substantially high.^{8,9} Further, the mass matrix pertaining to finite neutrino mass is not diagonal with respect to its various flavor species. As such, the mass eigenstates are not necessarily the flavor eigenstates, and may show mixing among its various flavor species.¹⁰ Mixings of Kobayashi-Maskawa¹¹ (KM) and hierarchical¹² type have been suggested and are being made use of in various investigations. Recent experiments have put some limits on some mixing matrices,^{2,13} yet their precise estimation shall require many more efforts in this direction.

A finite mass does not appear in $SU_L(2)\times U(1)$ electroweak theory in a natural way. They are introduced¹⁴ by adding (i) an additional Higgs scalar or (ii) an additional lepton or (iii) both. But in all these formulations a massive neutrino turns out to be of Majorana type. A massive neutrino occurs in a number of grand unified theories (GUT's), viz., in $SO(10)$ and E_6 , etc. In fact, in a recent paper Roy and Shanker¹⁵ have outlined a supersymmetric GUT $SO(10)$ scheme wherein Dirac neutrinos acquire masses. As such, ascertaining finite neutrino masses, mixing matrices, and oscillation phenomena is a necessity and may provide testing ground for GUT's with significant cosmological implications¹⁶ and hint towards the physics that exist beyond $SU(2)_L\times U(1)$ electroweak theory.

In order to detect effects pertaining to finite neutrino mass and mixings a number of processes such as β decay,^{6,7} muon decay,¹² τ^- decays,^{17,18} two-particle leptonic decays of mesons,^{19,20} and inner bremsstrahlung²¹ have been investigated with predictions that could possibly detect such contributions. Some phenomena such as the solar neutrino flux²² and beam-dump experiments²³ do not rule out the possibility of having such effects. At least

two experiments, namely, the one involving tritium decay⁶ and the Bugey-reactor oscillation experiment,²⁴ seem to give definite indications about the existence of finite neutrino mass and oscillations phenomena respectively.

In this work, we report our investigations on the three-particle semileptonic decays of K^+ . At present K^+ beam is copiously available at CERN in the proton-antiproton collider²⁵ (LEAR), and as such this facility may possibly be made use of for this purpose. The discussion makes use of the phenomenological $V-A$ theory^{12,16-19} with the inclusion of finite neutrino mass, treating neutrinos as Dirac particles. The use of the established $SU(2)_L\times U(1)$ theory¹⁴ and GUT's has purposely been avoided in this discussion of preliminary nature, as the latter are primarily expected to lead to refinements towards the predictions of this phenomenological discussion. In addition, Yukawa couplings involved in these models are not yet known.

The investigation focuses primarily on the following aspects of K_{l3}^+ decays: (i) Pion energy spectrum, (ii) decay probability and limits of ν_3 mass, (iii) $\pi-l$ ($=e,\mu$) angular correlations as a function of pion energy, (iv) $\pi-l$ energy correlations as a function of pion energy, (v) lepton energy spectrum, (vi) $\pi-\nu_i$ ($i=e,\mu,\tau$) angular correlations, and (vii) $\pi-\nu_i$ energy correlations as a function of pion energy.

The limits obtained on the ν_3 mass are consistent with presently known experimental upper bound.⁹ Finite- ν_3 -mass effects have a reasonable influence on all the parameters (i)-(vii). However, mixing contributions could be discernible only in pion-neutrino angular correlations and pion-neutrino energy correlations.

In the next section we give details of our discussion pertaining to all the aspects listed in (i)-(vii) and a summary of conclusions in Sec. III.

II. K_{l3}^+ DECAYSA. Pion energy spectrum in $K^+\rightarrow l+\nu_l\pi^0$

The matrix element²⁶ for the processes $K^+\rightarrow l+\nu_l\pi^0$, with the inclusion of the mixing matrix for neutrinos and radiative correction²⁷ is given by

$$M = \frac{G'}{\sqrt{2}} V_{12} \sum_i |U_{li}| \bar{u}_{\nu_i} [(p_K + p_\pi) f_+ + (p_K - p_\pi) f_-] \gamma^\lambda (1 - \gamma^5) V_l, \quad (1)$$

where G' is the coupling constant inclusive of radiative correction, U_{li} are the elements of neutrino-mass-mixing matrix with $l = e, \mu$ and $i = 1, 2, 3$, and V_{12} is the matrix element of the KM mixing matrix in quark sector.^{11,28}

The expression for the pion energy spectrum is obtained as

$$\frac{dW}{dx} = \frac{G'^2 V_{12}^2 \sum_i |U_{li}|^2 m_K^5 (x^2 - 4\delta_\pi^2)^{1/2} \lambda^{1/2} ((k-x), \delta_l^2, \delta_i^2) f_+^2}{384\pi^3 (k-x)^3} \\ \times ((x^2 - 4\delta_\pi^2)[2(k-x)^2 - (k-x)(\delta_l^2 + \delta_i^2) - (\delta_l^2 - \delta_i^2)^2] \\ + 3[(k-x)(\delta_l^2 + \delta_i^2) - (\delta_l^2 - \delta_i^2)^2] \{ (1 - \delta_\pi^2)^2 + (k-x)[(1 - \delta_\pi^2) + 2 \operatorname{Re} \xi + |\xi|^2 (k-x)] \}), \quad (2)$$

where

$$G'^2 = 1.021 G_\mu^2 \text{ (Ref. 27)}, \quad x = \frac{2E_\pi}{m_K}, \quad E_\pi = \text{energy of } \pi^0, \quad \delta_\pi^2 = \frac{m_{\pi^0}^2}{m_K^2}, \quad \delta_l^2 = \frac{m_l^2}{m_K^2}, \quad \delta_i^2 = \frac{m^2(\nu_i)}{m_K^2},$$

$$k = 1 + \delta_\pi^2, \quad \lambda(x, y, z) = x^2 + y^2 + z^2 - 2xy - 2yz - 2zx, \quad \xi = \frac{f_-}{f_+}, \quad \xi(0) = \xi \left[1 + \frac{\lambda + q^2}{m_\pi^2} \right],$$

$$f_+ = f_+(0) \left[1 + \frac{\lambda + q^2}{m_\pi^2} \right], \quad q^2 = (p_K - p_\pi)^2 \text{ (Refs. 29 and 30)}.$$

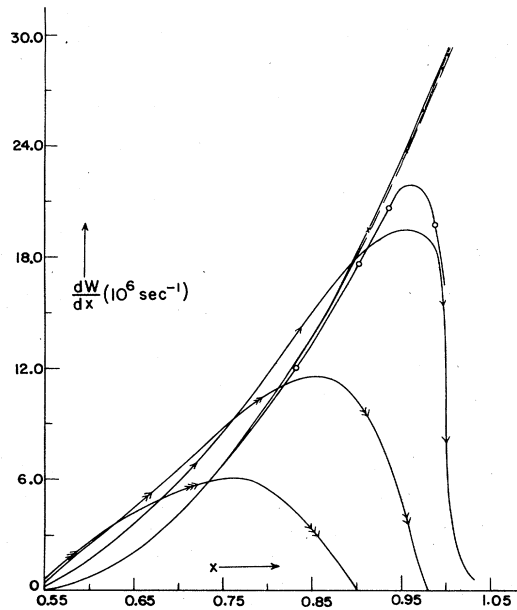


FIG. 1. Pion energy spectrum in the decay $K^+ \rightarrow e^+ \nu_i \pi^0$. Solid curve, single-arrow curve, double-arrow curve, and triple-arrow curve are for $m(\nu_3) = 0, 100, 150,$ and 200 MeV, respectively, without mixing. Dashed curve and single-circle curve are with KM mixing for $m(\nu_3) = 100$ and 200 MeV, respectively. Cross curve is for $m(\nu_3) = 100$ MeV with hierarchical mixing. Curves with hierarchical mixing (not shown) for $m(\nu_3) = 150$ and 200 MeV almost coincide with the curve of $m(\nu_3) = 0$.

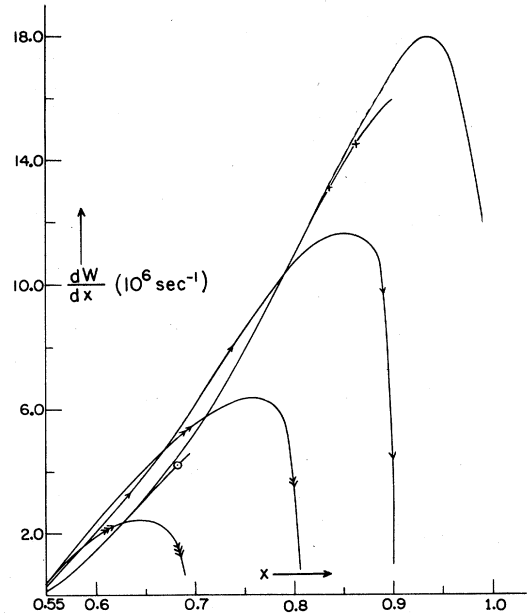


FIG. 2. Pion energy spectrum in the decay $K^+ \rightarrow \mu^+ \nu_i \pi^0$. Description of the curves is identical to that given in Fig. 1.

We take

$$f_+(0)V_{12}=0.2161 \text{ (Refs.27 and 28) ,}$$

$$\xi(0)=0, \lambda_+=0.0285\pm 0.0043$$

for K_{e3}^+ decays²⁹ and

$$\lambda_+=0.032\pm 0.008 ,$$

$$\xi(0)=-0.35\pm 0.15$$

for $K_{\mu 3}^+$ decays²⁹ for the purpose of numerical calculations.

Expression (2) shows that in general the pion energy spectrum for $l=e$ or μ , will be the sum of three different spectra for the cases $i=1,2,3$. Confining to the three-neutrino world, and, in order to have an order-of-magnitude estimate, we adopt the convention that the neutrino masses $m(\nu_i)$ are in ascending order of values, i.e., $m_1 < m_2 < m_3$. Further, for the case of nondegenerate neutrinos, we take ν_1, ν_2 , and ν_3 to be, respectively, ν_e, ν_μ , and ν_τ . Using the present experimental bounds on the masses of various neutrino species,⁶⁻⁹ $20 \text{ eV} < m(\nu_e) < 46 \text{ eV}$, $m(\nu_\mu) < 0.50 \text{ MeV}$, and $m(\nu_\tau) < 164 \text{ MeV}$, we obtain $\delta_1 < 9.32 \times 10^{-8}$, $\delta_2 < 1.01 \times 10^{-3}$, and $\delta_3 < 0.33$, where $\delta_i = m(\nu_i)/m_K$. Thus the dominant contribution comes from δ_3 only. Retaining δ_3 , we obtain for the pion energy spectrum, from Eq. (2), the expression

$$\begin{aligned} \frac{dW}{dx} = & \frac{G'^2 V_{12}^2 m_K^5 (x^2 - 4\delta_\pi^2)^{1/2} f_+^2}{384\pi^3 (k-x)^3} \\ & \times [(1 - U_{13}^2)(k-x - \delta_l^2)((x^2 - 4\delta_\pi^2)[2(k-x)^2 - \delta_l^2(k-x) - \delta_l^4] \\ & + 3[(k-x)\delta_l^2 - \delta_l^4]\{(1 - \delta_\pi^2)^2 + (k-x)[(1 - \delta_\pi^2)2\text{Re}\xi + |\xi|^2(k-x)]\}) \\ & + U_{13}^2 \lambda^{1/2}((k-x), \delta_l^2, \delta_3^2)((x^2 - 4\delta_\pi^2)[2(k-x)^2 - (k-x)(\delta_l^2 + \delta_3^2) - (\delta_l^2 - \delta_3^2)^2] \\ & + 3[(k-x)(\delta_l^2 + \delta_3^2) - (\delta_l^2 - \delta_3^2)^2] \\ & \times \{(1 - \delta_\pi^2)^2 + (k-x)[(1 - \delta_\pi^2)2\text{Re}\xi + |\xi|^2(k-x)]\})]. \end{aligned} \quad (3)$$

The pion energy spectrum in the decay $K^+ \rightarrow e^+ \pi^0 \nu_i$ is shown in Fig. 1 for $m(\nu_3)=0, 100, 150$, and 200 MeV . Matrices used for hierarchical¹² and KM (Ref. 5) mixings, respectively, are

$$|U_{ij}|^2 = \begin{bmatrix} 0.9947 & 0.005 & 0.0003 \\ 0.0043 & 0.9367 & 0.059 \\ 0.001 & 0.01 & 0.94 \end{bmatrix}, \quad (4)$$

$$|U_{ij}| = \begin{bmatrix} 0.95 & 0.22 & 0.21 \\ -0.23 & 0.97 & 0.04 \\ -0.21 & -0.08 & 0.98 \end{bmatrix}. \quad (5)$$

The effect of finite $m(\nu_3)$ on the pion energy spectrum throughout the pion energy range is substantial and becomes pronounced towards the high-energy end, i.e., for $x > 0.85$. Mixing effects are, however, negligible, the spectra involving hierarchical mixing are almost coincident with those for $m(\nu_3)=0$. KM mixing effects for $m(\nu_3)=200 \text{ MeV}$, for $x > 0.9$ may, however, be observable. The pion energy spectrum for the decay $K^+ \rightarrow \pi^0 \mu^+ \nu_i$, shown in Fig. 2, has qualitatively the same features as that for $K^+ \rightarrow e^+ \nu_i \pi^0$ except for numerical differences.

B. Decay probability and limits on ν_3 mass

The expression for the decay probability, obtained by integrating Eq. (3), is given by

$$\begin{aligned} W = & \frac{G'^2 V_{12}^2 m_K^5}{384\pi^3} \int_{x_{\min}}^{x_{\max}} \frac{f_+^2}{(k-x)^3} [(1 - U_{13}^2)(k-x - \delta_l^2)((x^2 - 4\delta_\pi^2)[2(k-x)^2 - \delta_l^2(k-x) - \delta_l^4] \\ & + 3[(k-x)\delta_l^2 - \delta_l^4] \\ & \times \{(1 - \delta_\pi^2)^2 + (k-x)[(1 - \delta_\pi^2)2\text{Re}\xi + |\xi|^2(k-x)]\}) \\ & + U_{13}^2 \lambda^{1/2}((k-x), \delta_l^2, \delta_3^2) \end{aligned}$$

$$\begin{aligned} &\times ((x^2 - 4\delta_\pi^2)[2(k-x)^2 - (k-x)(\delta_l^2 + \delta_3^2) - (\delta_l^2 - \delta_3^2)^2] \\ &+ 3[(k-x)(\delta_l^2 + \delta_3^2) - (\delta_l^2 - \delta_3^2)^2] \\ &\times \{(1 - \delta_\pi^2)^2 + (k-x)[(1 - \delta_\pi^2)2 \operatorname{Re}\xi + |\xi|^2(k-x)]\}) dx, \end{aligned} \tag{6}$$

where

$$x_{\max} = \frac{m_K^2 + m_{\pi^0}^2 - [m_l + m(\nu_i)]^2}{m_K^2},$$

and

$$x_{\min} = \frac{2m_{\pi^0}}{m_K}. \tag{7}$$

The variation of the decay probability with finite $m(\nu_3)$ for $l=e, \mu$ are shown in Figs. 3 and 4. Mixing effects are observable in the case of $K^+ \rightarrow e^+ \nu_i \pi^0$, but cannot be deciphered for $K^+ \rightarrow \mu^+ \nu_i \pi^0$ from those of finite $m(\nu_3)$.

Using experimental data²⁹ for K^+ decay time $= (1.2371 \pm 0.0026) \times 10^{-8}$ sec, and the branching fraction $= (4.82 \pm 0.05)$ percent, the experimental value of decay probability is found to be

$$W_{\text{expt}}(K^+ \rightarrow e^+ \nu_i \pi^0) = (3.90 \pm 0.041) \times 10^6 \text{ sec}^{-1}. \tag{8}$$

Giving different values to $m(\nu_3)$ in its theoretical expression (6) and comparing them with the experimental value [Eq. (8)], we calculate the value of $m(\nu_3)$ for which the two decay probabilities are equal. The values so obtained with the inclusion of hierarchical and KM mixing are given in Table I.

The corresponding value for the decay $K^+ \rightarrow \mu^+ \nu_i \pi^0$, with the use²⁹ of K^+ decay time $= (1.2371 \pm 0.0026) \times 10^{-8}$ sec and the branching fraction $= (3.20 \pm 0.09)$ percent, is found to be

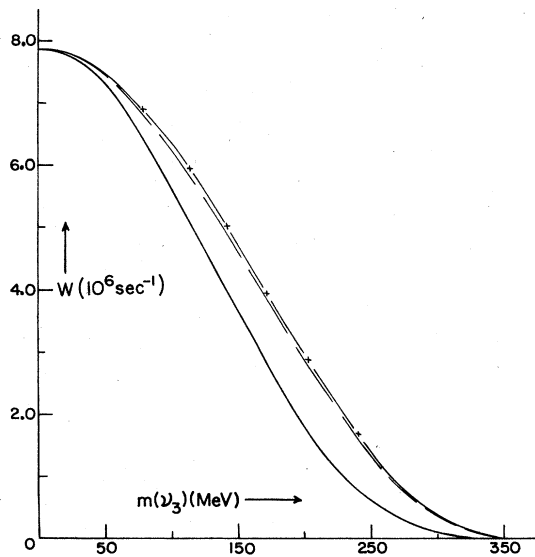


FIG. 3. Variation of decay probability with $m(\nu_3)$ in the decay $K^+ \rightarrow e^+ \nu_i \pi^0$. Solid curve, dashed curve, and cross curve are for without mixing, KM mixing, and hierarchical mixing, respectively.

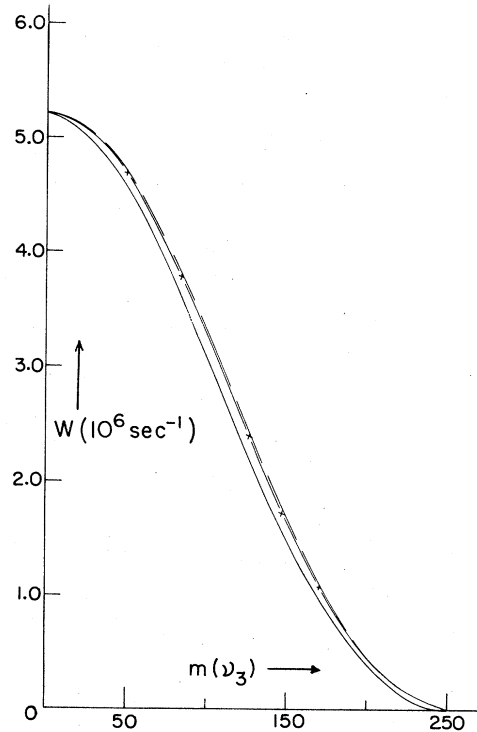


FIG. 4. Variation of decay probability with $m(\nu_3)$ in the decay $K^+ \rightarrow \mu^+ \nu_i \pi^0$. Description of the curves is identical to that given in Fig. 3.

$$W_{\text{expt}}(k^+ \rightarrow \mu^+ \nu_i \pi^0) = (2.59 \pm 0.07) \times 10^6 \text{ sec}^{-1}, \quad (9)$$

and the values of $m(\nu_3)$ calculated are given in Table I.

C. π - l angular correlations

The expression for the π - l angular correlation is obtained as

$$\begin{aligned} \frac{dW}{dx dz} = & \frac{G'^2 V_{12}^2 m_K^5 (x^2 - 4\delta_\pi^2)^{1/2}}{512\pi^3} \\ & \times \sum_{i=1}^3 \frac{|U_{ii}|^2 (y^2 - 4\delta_l^2) f_+^2}{[(2-x)(y^2 - 4\delta_l^2)^{1/2} + (x^2 - 4\delta_\pi^2)^{1/2} yz]} \\ & \times \{ [(2+x)(1 - \delta_\pi^2) + (x^2 - 4\delta_\pi^2)] 2y - y^2(2+x) \\ & + (x^2 - 4\delta_\pi^2)^{1/2} (y^2 - 4\delta_l^2)^{1/2} 2z [y(2+x) - (3 - \delta_\pi^2 + x)] - (x^2 - 4\delta_\pi^2)(y^2 - 4\delta_l^2) z^2 \\ & + 8\delta_l^2(k+x) + 2 \text{Re}\xi [(2+x)(k-x)2y - y^2(4-x^2) - (x^2 - 4\delta_\pi^2)^{1/2} (y^2 - 4\delta_l^2)^{1/2} 2z(xy + k - x) \\ & + (y^2 - 4\delta_l^2)(x^2 - 4\delta_\pi^2)z^2 + 8\delta_l^2(1 - \delta_\pi^2)] \\ & + |\xi|^2 \{ (2-x)(k-x)2y - y^2(2-x)^2 - (x^2 - 4\delta_\pi^2)^{1/2} (y^2 - 4\delta_l^2)^{1/2} 2z[(2-x)y - k + x] \\ & - (x^2 - 4\delta_\pi^2)(y^2 - 4\delta_l^2)z^2 + 8\delta_l^2(k-x) \} \}, \end{aligned} \quad (10)$$

where $z = \cos\theta_{\pi l}$,

$$\begin{aligned} y = & \frac{2E_l}{m_K} \\ = & \frac{2((k + \delta_l^2 - \delta_i^2 - x)(2-x) - (x^2 - 4\delta_\pi^2)^{1/2} z \{ (k + \delta_l^2 - \delta_i^2 - x)^2 - \delta_l^2 [(2-x)^2 - (x^2 - 4\delta_\pi^2)z^2] \}^{1/2})}{(2-x)^2 - (x^2 - 4\delta_\pi^2)z^2}, \end{aligned} \quad (11)$$

$\theta_{\pi l}$ will be in the range 0 to $\pi/2$. With the retention of dominant δ_3 contributions, the expression (10) reduces to the following:

$$\begin{aligned} \frac{dW}{dx dz} = & \frac{(1 - U_{13}^2) G'^2 V_{12}^2 m_K^5 (x^2 - 4\delta_\pi^2)^{1/2} (y_1^2 - 4\delta_l^2) f_+^2(0) [1 + \lambda_+(k-x)/\delta_\pi^2]^2}{512\pi^3 [(2-x)(y_1^2 - 4\delta_l^2)^{1/2} + (x^2 - 4\delta_\pi^2)^{1/2} y_1 z]} \\ & \times \left\{ [(2+x)(1 - \delta_\pi^2) + (x^2 - 4\delta_\pi^2)] 2y_1 - y_1^2(2+x)^2 + (x^2 - 4\delta_\pi^2)^{1/2} (y_1^2 - 4\delta_l^2)^{1/2} 2z [y_1(2+x) - (3 - \delta_\pi^2 + x)] \right. \\ & - (x^2 - 4\delta_\pi^2)(y_1^2 - 4\delta_l^2)z^2 + 8\delta_l^2(k+x) \\ & \left. + 2\xi(0) \left[1 - \lambda_+ \frac{k-x}{\delta_\pi^2} \right] [(2+x)(k-x)2y_1 - y_1^2(4-x)^2 - (x^2 - 4\delta_\pi^2)^{1/2} (y_1^2 - 4\delta_l^2)^{1/2} 2z(xy_1 + k - x) \right. \right. \\ & \left. \left. + (y_1^2 - 4\delta_l^2)(x^2 - 4\delta_\pi^2)z^2 + 8\delta_l^2(1 - \delta_\pi^2)] \right\} \end{aligned}$$

$$\begin{aligned}
& + \xi^2(0) \left[1 - \lambda_+ \frac{k-x}{\delta_\pi^2} \right]^2 \left\{ (2-x)(k-x)2y_1 - y_1^2(2-x)^2 - (x^2 - 4\delta_\pi^2)^{1/2}(y_1^2 - 4\delta_l^2)^{1/2}2z[(2-x)y_1 - k + x] \right. \\
& \quad \left. - (x^2 - 4\delta_\pi^2)(y_1^2 - 4\delta_l^2)z^2 + 8\delta_l^2(k-x) \right\} \\
& + \frac{U_{13}^2 G'^2 V_{12}^2 m_K^5 (x^2 - 4\delta_\pi^2)^{1/2} (y^2 - 4\delta_l^2) f_+^2(0)}{512\pi^3 [(2-x)(y^2 - 4\delta_l^2)^{1/2} + (x^2 - 4\delta_\pi^2)^{1/2}yz]} \left[1 + \lambda_+ \frac{k-x}{\delta_\pi^2} \right]^2 \\
& \times [\text{all the above terms of this expression with the replacement } y_1 \rightarrow y], \tag{12}
\end{aligned}$$

where

$$y_1 = \frac{2((k + \delta_l^2 - x)(2-x) - (x^2 - 4\delta_\pi^2)^{1/2}z\{(k + \delta_l^2 - x)^2 - \delta_l^2[(2-x)^2 - (x^2 - 4\delta_\pi^2)z^2]\}^{1/2})}{(2-x)^2 - (x^2 - 4\delta_\pi^2)z^2},$$

and

$$y = \frac{2((k + \delta_l^2 - \delta_3^2 - x)(2-x) - (x^2 - 4\delta_\pi^2)^{1/2}z\{(k + \delta_l^2 - \delta_3^2 - x) - \delta_l^2[(2-x)^2 - (x^2 - 4\delta_\pi^2)z^2]\}^{1/2})}{(2-x)^2 - (x^2 - 4\delta_\pi^2)z^2}. \tag{13}$$

The π - l angular correlations for $l=e$ and μ are shown, respectively, in Figs. 5 and 6 for $m(\nu_3)=0, 100, 150,$ and 200 MeV. Finite- $m(\nu_3)$ effects are precisely transparent in numerical values, whereas the qualitative variation is identical to that with $m(\nu_3)=0$. Mixing effects are, however, very small.

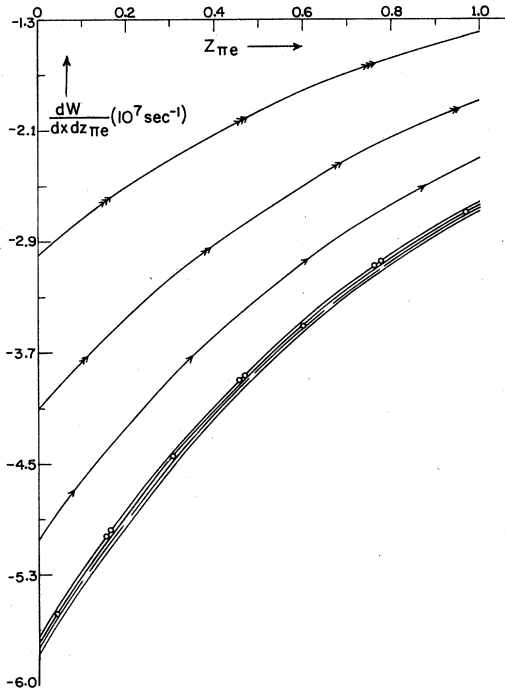


FIG. 5. π - e angular correlation in the decay $K^+ \rightarrow e^+ \nu_i \pi^0$. Solid curve, single-arrow curve, double-arrow curve, and triple-arrow curve, are, respectively, for $m(\nu_3)=0, 100, 150,$ and 200 MeV without mixing. Dashed curve, single-circle curve, and double-circle curve are, respectively, for $m(\nu_3)=100, 150,$ and 200 MeV with KM mixing. Curves for $m(\nu_3)=100, 150,$ and 200 MeV with hierarchical mixing (not shown) are almost coincident with the solid curve for $m(\nu_3)=0$.

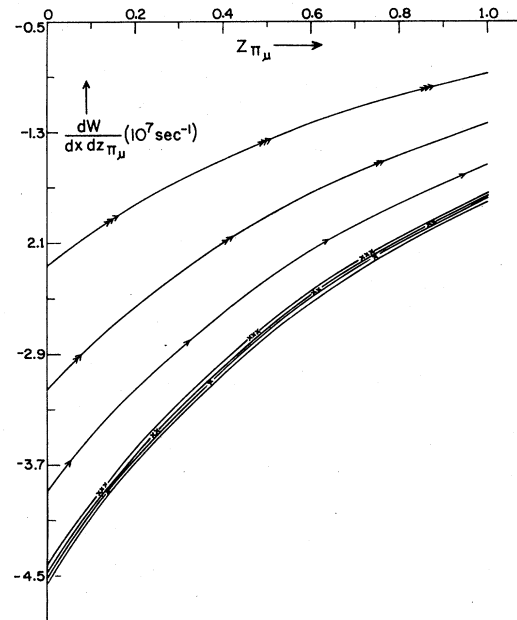


FIG. 6. π - μ angular correlation in the decay $K^+ \rightarrow \mu^+ \nu_i \pi^0$. Single-cross, double-cross, and triple-cross curves are, respectively, for $m(\nu_3)=100, 150,$ and 200 MeV, with hierarchical mixing. The description of other curves is identical to that given in Fig. 5. Curves, not shown in figure, for $m(\nu_3)=100, 150,$ and 200 MeV, with KM mixing, almost coincide with the solid curve.

D. π - l energy correlations

The expression for π - l energy correlations is

$$\frac{dW}{dx dy} = \frac{\sum_{i=1}^3 |U_{li}|^2 G^{\prime 2} V_{12}^2 m_K^5 f_+^2(0) \left[1 + \lambda_+ \frac{k-x}{\delta_\pi^2} \right]^2}{128\pi^3} \times \left[\begin{aligned} & [(2+x)(1-\delta_\pi^2) + (x^2 - 4\delta_\pi^2)] 2y - y^2(2+x)^2 + 2(x^2 - 4\delta_\pi^2)^{1/2} (y^2 - 4\delta_l^2)^{1/2} \cos\theta_{\pi l} [y(2+x) - 3 + \delta_\pi^2 - x] \\ & - (x^2 - 4\delta_\pi^2)(y^2 - 4\delta_l^2) \cos^2\theta_{\pi l} + 8\delta_l^2(k+x) \\ & + 2\xi(0) \left[1 - \lambda_+ \frac{k-x}{\delta_\pi^2} \right] [2y(2+x)(k-x) - y^2(4-x^2) - 2(x^2 - 4\delta_\pi^2)^{1/2} (y^2 - 4\delta_l^2)^{1/2} \cos\theta_{\pi l} (k-x+xy) \\ & \quad + (x^2 - 4\delta_\pi^2)(y^2 - 4\delta_l^2) \cos^2\theta_{\pi l} + 8\delta_l^2(1-\delta_\pi^2)] \\ & + \xi^2(0) \left[1 - \lambda_+ \frac{k-x}{\delta_\pi^2} \right]^2 \{ (k-x)(2-x) 2y - y^2(2-x)^2 \\ & \quad + 2(x^2 - 4\delta_\pi^2)^{1/2} (y^2 - 4\delta_l^2)^{1/2} \cos\theta_{\pi l} [k-x-y(2-x)] \\ & \quad - (x^2 - 4\delta_\pi^2)(y^2 - 4\delta_l^2) \cos^2\theta_{\pi l} + 8\delta_l^2(k-x) \} \end{aligned} \right], \quad (14)$$

with $x = 2E_{\pi^0}/m_K$, $y = 2E_l/m_K$, and

$$\cos\theta_{\pi l} = \frac{2(k-x + \delta_l^2 - \delta_\pi^2) - y(2-x)}{(x^2 - 4\delta_\pi^2)^{1/2} (y^2 - 4\delta_l^2)^{1/2}}. \quad (15)$$

Again retaining the contributions from the δ_3 term in Eq. (14), we plot $dW/dx dy$ versus x in Figs. 7 and 8 for e and μ decays, respectively. Here again the finite- $m(\nu_3)$ effects are observable and mixing contributions are negligible.

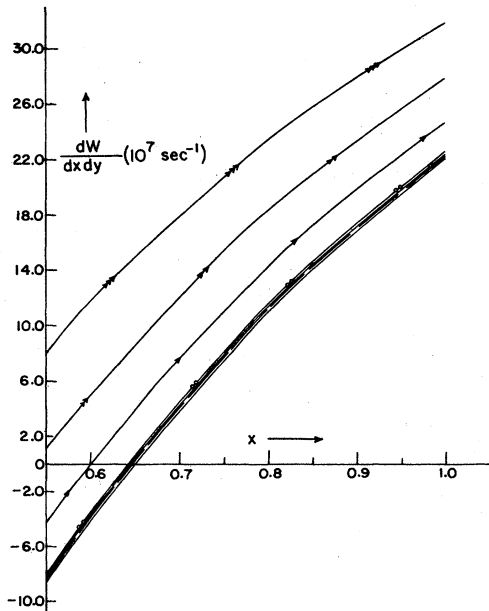


FIG. 7. π - e energy correlation in the decay $K^+ \rightarrow e^+ \nu_i \pi^0$. Description of the curves is identical to that given in Fig. 5.

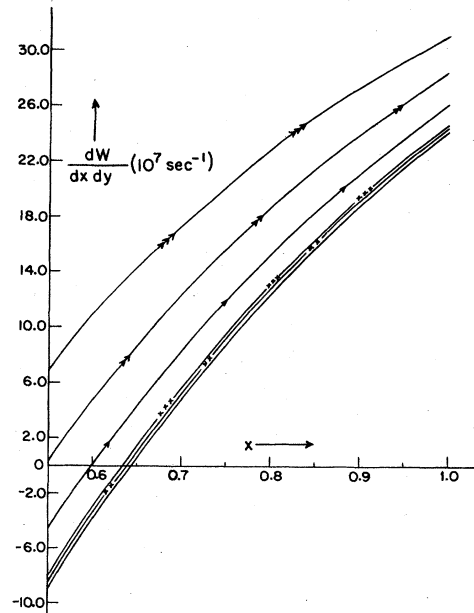


FIG. 8. π - μ energy correlation in the decay $K^+ \rightarrow \mu^+ \nu_i \pi^0$. Description of the curves is identical to that in Fig. 6.

E. Lepton energy spectrum in $K^+ \rightarrow l^+ \nu_l \pi^0$

Integration of Eq. (14) for x gives the expression for lepton energy spectrum

$$\begin{aligned} \frac{dW}{dy} = & \frac{\sum_{i=1}^3 |U_{li}|^2 G^2 V_{12}^2 f_+^2(0) m_K^5}{128\pi^3} \\ & \times \int_{x_{\min}}^{x_{\max}} \left[1 + \lambda_+ \frac{k-x}{\delta_\pi^2} \right]^2 \left\{ (2+x)(1-\delta_\pi^2) + (x^2 - 4\delta_\pi^2) \right\} 2y - y^2(2+x)^2 \\ & + [2(k-x + \delta_l^2 - \delta_i^2) - y(2-x)] [y(6+x) - 2(4 + \delta_l^2 - \delta_i^2)] + 8\delta_l^2(k+x) \\ & + 2\xi(0) \left[1 - \lambda_+ \frac{k-x}{\delta_\pi^2} \right] \left\{ 2y(2+x)(k-x) - y^2(4-x^2) \right. \\ & \quad \left. + [2(k-x + \delta_l^2 - \delta_i^2) - y(2-x)](2\delta_l^2 - 2\delta_i^2 - xy - 2y) \right. \\ & \quad \left. + 8\delta_l^2(1 - \delta_\pi^2) \right\} \\ & + \xi^2(0) \left[1 - \lambda_+ \frac{k-x}{\delta_\pi^2} \right]^2 \left\{ (k-x)(2-x)2y - y^2(2-x)^2 \right. \\ & \quad \left. + [2(k-x + \delta_l^2 - \delta_i^2) - y(2-x)](xy - 4y + 2\delta_l^2 + 2\delta_i^2) \right. \\ & \quad \left. + 8\delta_l^2(k-x) \right\} dx, \end{aligned} \tag{16}$$

where x_{\max} and x_{\min} are given by Eq. (7). Retaining again the dominant contribution from the δ_3 term, we show the variation of dW/dy with y , $l=e$ and μ , respectively, in Figs. 9 and 10. The finite- $m(\nu_3)$ effects are distinct and that of mixing can be observable for $0.45 < y < 0.65$, and $y < 0.15$. The distinction between hierarchical and KM mixings is, however, not possible.

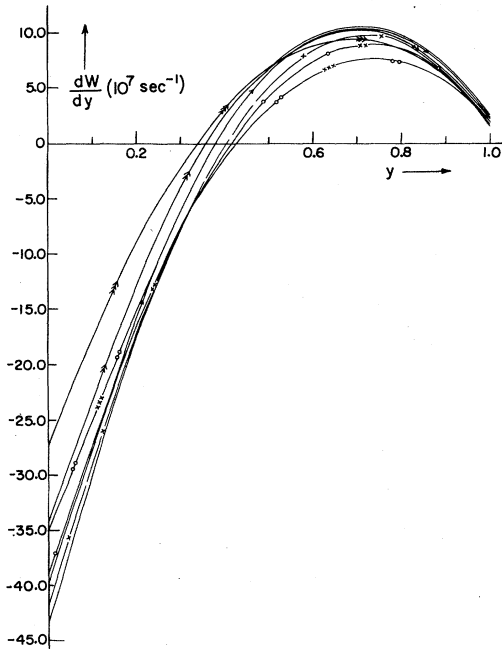


FIG. 9. Electron energy spectrum in the decay $K^+ \rightarrow e^+ \nu_l \pi^0$. Description of the curves is identical to that given in Figs. 5 and 6.

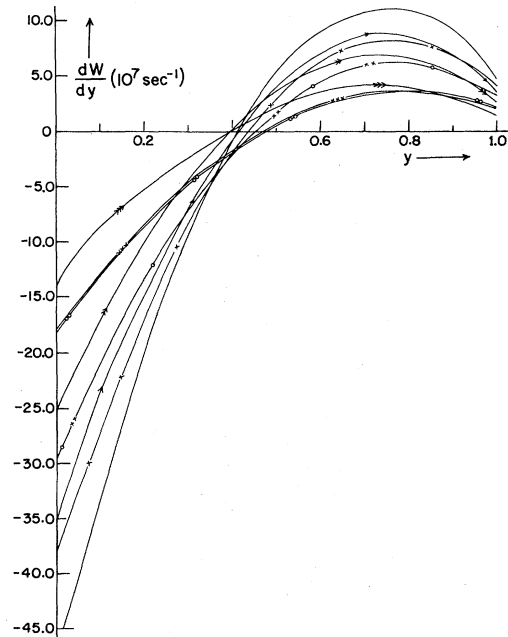


FIG. 10. Muon energy spectrum in the decay $K^+ \rightarrow \mu^+ \nu_l \pi^0$. Description of the curves is identical to that given in Figs. 5 and 6.

F. π - ν_i angular correlations

The expressions for pion-neutrino angular correlations are obtained from Eq. (10) by making the replacements $m_l \leftrightarrow m(\nu_i)$, $E_l \rightarrow E_{\nu_i}$, $\theta_{\pi l} \rightarrow \theta_{\pi \nu_i}$, and $\sum |U_{li}|^2 \rightarrow |U_{li}|^2$:

$$\begin{aligned} \frac{dW}{dx dz} = & \frac{|U_{li}|^2 G'^2 V_{12}^2 f_+^2(0)(x^2 - 4\delta_\pi^2)^{1/2}(y^2 - 4\delta_i^2) m_K^5 \left[1 + \lambda_+ \frac{k-x}{\delta_\pi^2} \right]^2}{512\pi^3 [(2-x)(y^2 - 4\delta_i^2)^{1/2} + (x^2 - 4\delta_\pi^2)^{1/2} z y]} \\ & \times \left[[(1 - \delta_\pi^2)(2+x) + (x^2 - 4\delta_\pi^2)] 2y - y^2(2+x)^2 \right. \\ & + 2(x^2 - 4\delta_\pi^2)^{1/2}(y^2 - 4\delta_i^2)^{1/2} z [y(2+x) - 3 + \delta_\pi^2 - x] - (x^2 - 4\delta_\pi^2)(y^2 - 4\delta_i^2) z^2 + 8\delta_i^2(k+x) \\ & + 2\xi^2(0) \left[1 - \lambda_+ \frac{k-x}{\delta_\pi^2} \right] [(k-x)(2+x)2y - y^2(4-x^2) - 2(x^2 - 4\delta_\pi^2)^{1/2}(y^2 - 4\delta_i^2)^{1/2} z(xy + k-x) \\ & \quad \left. + (x^2 - 4\delta_\pi^2)(y^2 - 4\delta_i^2) z^2 + 8\delta_i^2(1 - \delta_\pi^2)] \right] \\ & + \xi^2(0) \left[1 - \lambda_+ \frac{k-x}{\delta_\pi^2} \right]^2 \left\{ (k-x)(2-x)2y - y^2(2-x)^2 + 2(x^2 - 4\delta_\pi^2)^{1/2}(y^2 - 4\delta_i^2)^{1/2} z [k-x - y(2-x)] \right. \\ & \quad \left. - (x^2 - 4\delta_\pi^2)(y^2 - 4\delta_i^2) z^2 + 8\delta_i^2(k-x) \right\} \Bigg], \end{aligned} \quad (17)$$

where

$$y = \frac{2E_{\nu_i}}{m_K} = \frac{2((k + \delta_i^2 - \delta_l^2 - x)(2-x) \pm (x^2 - 4\delta_\pi^2)^{1/2} z \{ (k + \delta_i^2 - \delta_l^2 - x)^2 - \delta_i^2 [(2-x)^2 - (x^2 - 4\delta_\pi^2) z^2] \}^{1/2})}{(2-x)^2 - (x^2 - 4\delta_\pi^2) z^2} \quad (18)$$

and

$$z = \cos \theta_{\pi \nu_i}.$$

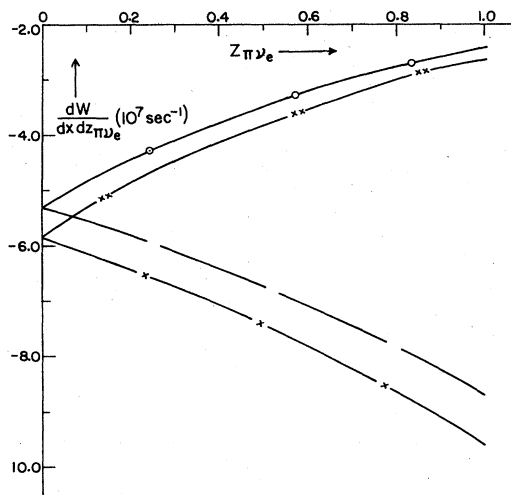


FIG. 11. π - ν_e angular correlation in the decay $K^+ \rightarrow e^+ \nu_i \pi^0$. Single-cross and double-cross curves are for hierarchical mixing with y_{\max} and y_{\min} , respectively. Dashed curve and single-circle curve are for KM mixing with y_{\max} and y_{\min} , respectively (see text).

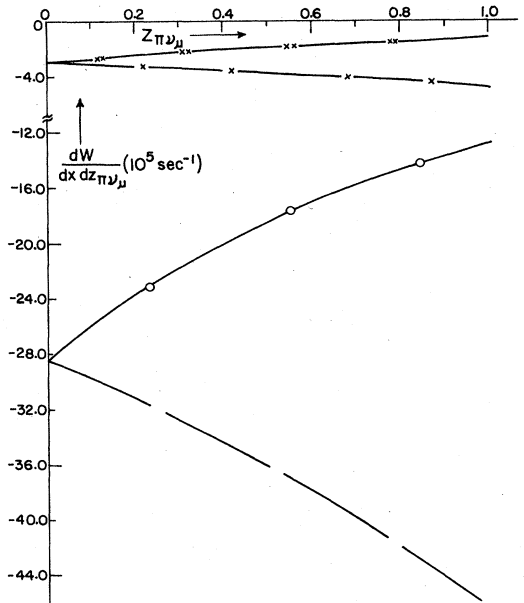


FIG. 12. π - ν_μ angular correlation in the decay $K^+ \rightarrow e^+ \nu_i \pi^0$. Description of the curves is identical to that given in Fig. 11.

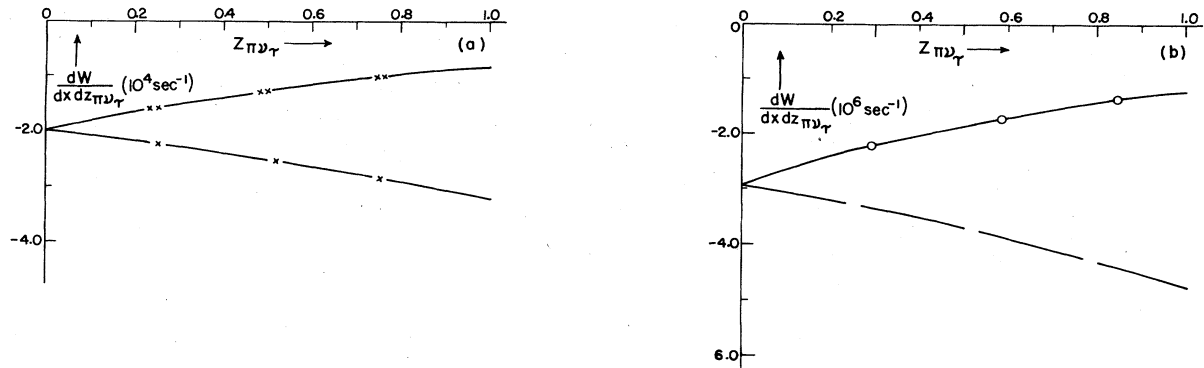


FIG. 13. π - ν_τ angular correlation in the decay $K^+ \rightarrow e^+ \nu_i \pi^0$. (a) Single-cross curve and double-cross curve are for hierarchical mixing with y_{\max} and y_{\min} , respectively (see text). (b) Dashed curve and single-circle curve are for KM mixing with y_{\max} and y_{\min} , respectively (see text).

Variations of $dW/dx dz$ with $z = z_{\pi\nu_e}$, $z_{\pi\nu_\mu}$, and $z_{\pi\nu_\tau}$ in the decay $K^+ \rightarrow e^+ \nu_i \pi^0$ are shown in Figs. 11–13, respectively, for the dominant mode taking $m(\nu_e) = m(\nu_\mu) = 0$, $m(\nu_3) = 150$ MeV, and $x = 0.6$. It is seen that mixings contribute significantly towards these correlations. In this case one may also discern between the types of mixing used.

Corresponding angular correlations in the decay $K^+ \rightarrow \mu^+ \nu_i \pi^0$, give almost identical qualitative spectrum but with obvious numerical differences. However, it is very difficult to differentiate between KM and hierarchical mixing in π - ν_μ angular correlation of this decay.

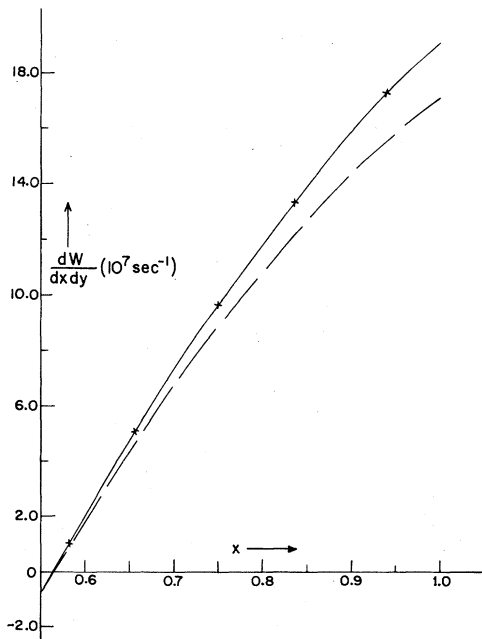


FIG. 14. π - ν_e energy correlation in the decay $K^+ \rightarrow e^+ \nu_i \pi^0$. Single-cross curve and dashed curve are for hierarchical and KM mixing, respectively (see text).

G. π - ν_i energy correlations in $K^+ \rightarrow l^+ \nu_i \pi^0$

The expression for π - ν_i energy correlations are obtained from Eqs. (14) and (15) by making the replacements $m_l \leftrightarrow m(\nu_i)$, $E_l \rightarrow E_{\nu_i}$, $\theta_{\pi l} \rightarrow \theta_{\pi\nu_i}$, and $\sum_{i=1}^3 |U_{li}|^2 = |U_{li}|^2$.

π - ν_e , π - ν_μ , and π - ν_τ energy correlations in the decay $K^+ \rightarrow e^+ \nu_i \pi^0$ are shown, respectively, in Figs. 14–16, taking $m(\nu_e) = m(\nu_\mu) = 0$, $m(\nu_3) = 150$, and $y = 0.65$. Here again one notices the distinct contributions from mixing and also the distinction between hierarchical and KM mixing contributions in π - ν_μ and π - ν_τ energy correlations. However, this is very small in π - ν_e energy correlations.

For the decay $K^+ \rightarrow \mu^+ \nu_i \pi^0$, the qualitative nature of π - ν_i energy correlations is almost identical to that for electronic decay. But in this case the difference in the nature of mixing is very small for π - ν_μ energy correlation and is distinct in π - ν_e and π - ν_τ energy correlations.

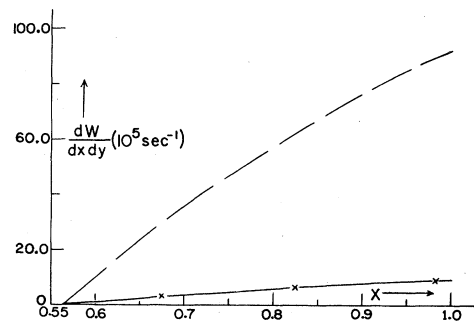


FIG. 15. π - ν_μ energy correlation in the decay $K^+ \rightarrow e^+ \nu_i \pi^0$. Description of the curves is identical to that given in Fig. 14.

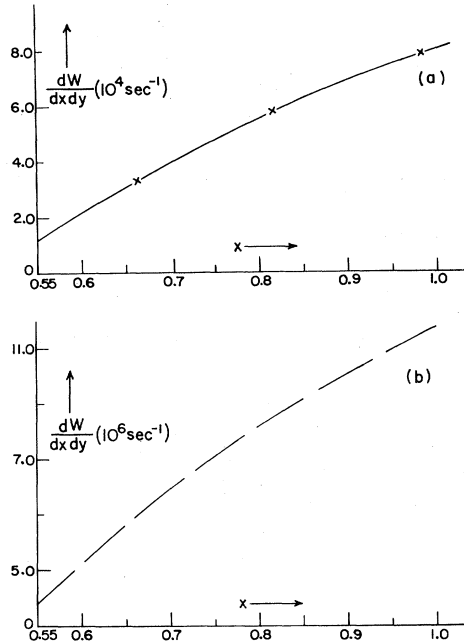


FIG. 16. π - ν_τ energy correlation in the decay $K^+ \rightarrow e^+ \nu_i \pi^0$, (a) with hierarchical mixing, (b) with KM mixing.

III. SUMMARY AND CONCLUSIONS

(1) The contributions of finite $m(\nu_3)$ are substantial in (i) pion energy spectrum, (ii) π - l angular correlations, (iii)

π - l energy correlations, and (iv) lepton energy spectrum. The effect becomes pronounced in the pion energy spectrum towards the high-energy tail ($x > 0.85$).

(2) The neutrino-mass-mixing effects are, in general, very small in (i) pion energy spectrum, (ii) π - l angular correlations, and (iii) π - l energy correlations. However, in the pion energy spectrum it could be reasonable towards the high-energy end ($x > 0.9$) and for higher value of $m(\nu_3)$. The mixing effects are pronounced in π - ν_i angular and energy correlations. As such, correlation studies³¹ could be a useful place for ascertaining such contributions, and possibly the values of mixing parameters.

(3) The ν_3 mass limits, calculated for the two decays by using the present values of experimental parameters, are consistent with the recently reported upper-bound $m(\nu_3) < 164$ MeV. It may, however, be pointed out that in models involving massive neutrinos, neutrinos involving still higher-mass species¹³ are not ruled out, notwithstanding the constraints provided by cosmological considerations.³²

Finally, the discussion reported in this work does point towards the fact that K_{l3}^+ decays may be a useful place to look for finite-neutrino-mass contributions and possibly the mass-mixing effects too.

ACKNOWLEDGMENTS

The authors wish to express their sincere thanks to Professor S. Lokanathan for useful discussions. R.R.L.S. is grateful to University Grants Commission (India) for providing him financial assistance.

*On academic leave from Government College, Dholpur, Rajasthan, India.

¹See, for instance, *Proceedings of the Neutrino Mass Workshop, Telemark, Wisconsin, 1980*, edited by V. Barger and D. Cline (University of Wisconsin, Madison, Report No. UW-186, 1980); A. De Rújula, in *Proceedings of the Ninth International Conference on High Energy Physics and Nuclear Structure, Versailles, 1981*, edited by P. Catillon, P. Radvanyi, and M. Porneuf [Nucl. Phys. **A374**, 619c (1982)]; A. De Rújula and M. Lusignoli, CERN Report No. TH. 3300, 1982 (unpublished).

²F. Bergsma *et al.*, CERN-Hamburg-Amsterdam-Rome-Moscow (CHARM) Collaboration, Phys. Lett. **128B**, 361 (1983).

³R. N. Mohapatra and G. Senjanovic, Phys. Rev. D **23**, 165 (1983).

⁴V. Barger, K. Whisnant, and R. J. N. Phillips, Phys. Rev. D **22**, 1636 (1980).

⁵D. Silverman and A. Soni, Phys. Rev. D **27**, 58 (1983).

⁶S. Boris *et al.*, to be published, quoted by V. A. Lubimov, in *Proceedings of the International Europhysics Conference on High Energy Physics, Brighton, 1983*, edited by J. Guy and C. Costain (Rutherford Appleton Laboratory, Chilton, Didcot, United Kingdom, 1984). See also V. A. Lubimov *et al.*, Phys. Lett. **94B**, 266 (1980).

⁷K. E. Bergkvist, Nucl. Phys. **B39**, 317 (1972).

⁸D. C. Lu *et al.*, Phys. Rev. Lett. **45**, 1066 (1980); M. Duam

et al., Phys. Rev. D **20**, 2692 (1979); M. LeCoutre *et al.*, in *Proceedings of Moriond Workshop, La Plagne, France, 1984* (unpublished).

⁹C. Matteuzzi *et al.*, Phys. Rev. Lett. **52**, 1869 (1984).

¹⁰See, for example, Ta-Pei Cheng and Ling-Fong Li, *Gauge Theories of Elementary Particles* (Clarendon, Oxford, 1984), pp. 357–359.

¹¹M. Kobayashi and K. Maskawa, Prog. Theor. Phys. **49**, 652 (1973).

¹²P. Kalyniak and John N. Ng, Phys. Rev. D **24**, 1874 (1981).

¹³F. Vannucci, CERN Report No. EP 84-104, 1984 (unpublished).

¹⁴T. P. Cheng and Ling-Fong Li, Phys. Rev. D **22**, 2860 (1980); J. Schechter and J. W. F. Valle, *ibid.* **22**, 2227 (1980).

¹⁵P. Roy and O. Shanker, Phys. Rev. Lett. **52**, 713 (1984); also see D. Wyler and L. Wolfstein, Nucl. Phys. **B218**, 205 (1983), who have given a somewhat different treatment of a similar scheme.

¹⁶G. Steigman, in *Physics at Very High Energies*, proceedings of the SLAC Summer Institute on Particle Physics, 1982, edited by Anne Mosher (SLAC Report No. 259, 1983), pp. 651–666.

¹⁷R. R. L. Sharma and N. K. Sharma, Pramana **21**, 329 (1983).

¹⁸R. R. L. Sharma and N. K. Sharma, Phys. Rev. D **29**, 1533 (1984); **30**, 2418 (1984); J. Babson and Ernest Ma, Z. Phys. C **20**, 5 (1983).

¹⁹R. E. Shrock, Phys. Lett. **96B**, 159 (1980).

²⁰R. E. Shrock, Phys. Rev. D **24**, 1232 (1981).

- ²¹A. De Rújula, Nucl. Phys. **B188**, 414 (1981).
- ²²R. Davis *et al.*, Report No. BNL-24629, 1978 (unpublished); R. Davis, in *Proceedings of the Neutrino Mass Workshop, Telemark, Wisconsin, 1980* (Ref. 1).
- ²³F. Dydak, in *Neutrino Physics and Astrophysics*, proceedings of the International Conference, Erice, 1980, edited by E. Fiorini (Plenum, New York, 1981).
- ²⁴J. F. Cavaignac *et al.*, LAPP Report No. LAPP-Exp.-84-03 (unpublished); Report No. ISN-84-11, 1984 (unpublished).
- ²⁵R. Decker, P. Pavlopoulos, and G. Zoupanos, CERN Report No. TH.3917, 1984 (unpublished).
- ²⁶E. D. Commins, *Weak Interactions* (McGraw-Hill, New York, 1973), pp. 225–234.
- ²⁷H. Leutwyler and M. Roos, CERN Report No. TH.3830, 1984 (unpublished).
- ²⁸R. E. Shrock and L. L. Wang, Phys. Rev. Lett. **41**, 1692 (1978).
- ²⁹Particle Data Group, Phys. Lett. **111B**, 1 (1982).
- ³⁰L. M. Chounet, J. M. Gaillard, and M. K. Gallard, Phys. Rep. **4C**, 199 (1972).
- ³¹*Advances in Particle Physics*, edited by R. L. Cool and R. E. Marshak (Interscience, New York, 1968), Vol. 1, pp. 313–317.
- ³²S. Sarkar and A. M. Cooper, Reports Nos. CERN-TH.3976/84 and CERN/EP 84-97 (unpublished).